Cation-Binding Sites of Subtilisin Carlsberg Probed with Eu(III) Luminescence

Sunbae Lee and Du-Jeon Jang
School of Chemistry and Molecular Engineering, Seoul National University, Seoul 151-742, Korea

ABSTRACT Two Ca^{2+}-binding sites of subtilisin Carlsberg are studied by monitoring static and time-resolved luminescence of selectively substituted Eu^{3+} at each site, and they are found to be characteristically quite different from each other. Compared with the coordination sphere of free Eu^{3+}, two sites are very similar to each other, so that both have a well-defined binding structure with low coordination symmetry. However, compared with the weak site, the strong site is relatively more polar, more symmetrical, and more easily accessible. Furthermore, despite the absence of water reported in the x-ray crystal structure (Bode et al., 1987, *Eur. J. Biochem.* 166:673–692), one water molecule is found to exist in the coordination sphere of the strong site in aqueous solution. Thus it is suggested that in solution the Ca^{2+} bound in the strong site forms an additional coordination bond to a solvent or substrate molecule.

INTRODUCTION

Subtilisins comprise a group of serine endopeptidases that are secreted in large amounts from a wide variety of *Bacillus* species. Serine proteases, present in virtually all organisms, exist as two families, the "trypsin-like" and the "subtilisin-like," that have independently evolved a similar catalytic device characterized by the triad of Ser, His, and Asp (Carter and Wells, 1988). The subtilisins are of considerable interest not only scientifically but also industrially, for they are used in such diverse applications as meat tenderizers, laundry detergents, and proteolytic medicines (Genov et al., 1995; Fitzpatrick et al., 1994). Furthermore, recent research on catalytic efficiency and specificity in organic solvents has enhanced their practical utility in synthetic applications (Broos et al., 1995; Chatterjee and Russell, 1993; Chaudhary et al., 1996; Kijima et al., 1994). There have been many studies made of their stability (Pantoliano et al., 1989; Siezen et al., 1991; Strausberg et al., 1993), as stabilization normally improves their properties for applications. In many enzymes, metal ions have been reported to play an important role in stabilizing proteins by binding at specific sites (Genov et al., 1995). One well-known example is thermolysin, a neutral protease, which is known to contain four Ca^{2+}-binding sites. The additional contribution of four Ca^{2+} binding is collectively as high as 9 kcal/mol in the free energy of unfolding (Voordouw et al., 1976). So information on the structural and functional roles of metal ion-binding sites is very important from the standpoint of industrial applications as well as academic interest.

Subtilisin Carlsberg (sC), secreted by *Bacillus licheniformis* (Smith et al., 1968), is a single polypeptide chain of 274 amino acid residues with two Ca^{2+} ion-binding sites (Bode et al., 1987; McPhalen and James, 1988; Neidhart and Petsko, 1988). The x-ray structure of the strong site with a binding constant of 10^8 (Pantoliano et al., 1989) has an approximately octahedral coordination sphere with three carbonyls, two carboxyamides, and one carboxylate (Bode et al., 1987; McPhalen and James, 1988; Neidhart and Petsko, 1988). On the other hand, the weak site, with a binding constant of 10^2 (Pantoliano et al., 1988), has a quadrangular pyramidal structure with three peptide carbonyl groups and two water molecules (Bode et al., 1987; McPhalen and James, 1988). However, it is noteworthy that the binding site surroundings of crystalline sC, prepared for x-ray measurements, could be quite different from those of in situ sC. Ca^{2+} ion binding is known to slow down autolysis and to enhance thermal stability (Pantoliano et al., 1988). A recent report on the subtilisin BPN′, which is similar to sC in structure, indicates that Ca^{2+} binding at the weak site as well as at the strong site enhances protein stability dramatically (Kidd et al., 1996).

Rare earth cations are extensively utilized in the fields of biology, chemistry, and earth science to solve a variety of structural and analytical problems (Bunzli and Choppin, 1989; Choppin and Peterman, 1998; Lee et al., 1999; Pucker et al., 1996). Their luminescence is highly efficient, but, in addition, their spectrum, quantum yield, and lifetime are sensitive to their environment. In particular, Eu luminescence is remarkably valuable. Excitation to the strongly allowed $^5L_6$ level from the ground $^7F_0$ level leads the Eu^{3+} ion to the $^5D_0$ level via fast nonradiative relaxation processes at room temperature, before radiative relaxation to one of the ^7F_J ($J = 0$ to 6) levels (Fig. 1). The luminescence bands that are mainly monitored in this report are the transition bands of $^5D_0 \rightarrow {}^7F_1$ (F_1) and $^5D_0 \rightarrow {}^7F_2$ (F_2). The electric dipole transition of F_2 in a symmetry with an inversion center is forbidden by parity (Bunzli and Choppin, 1989; Choppin and Peterman, 1998). However, interactions with the ligand field or with vibrational states mix electronic states of different parities, and the transition arising from

Received for publication 10 March 2000 and in final form 30 June 2000.
Address reprint requests to Dr. Du-Jeon Jang, School of Chemistry, Seoul National University, Seoul 151-742, Korea. Tel.: 82-2-875-6624; Fax: 82-2-889-1568; E-mail: djjang@plaza.snu.ac.kr.

0006-3495/00/10/2171/07 $2.00

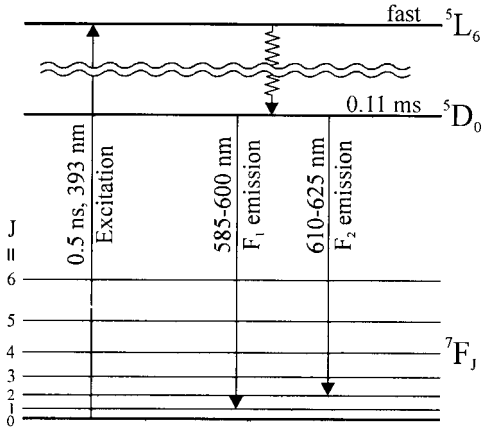

FIGURE 1 Schematic energy levels and their relaxation dynamics of aqueous Eu^{3+} at room temperature (Bunzli and Choppin, 1989), showing the transition bands that were mainly used for excitation and emission.

this hybridization is called a forced electric dipole transition. As the forced transition of F_2 is originating from interactions with neighbors, it is hypersensitive to environmental effects (Oomen and van Dongen, 1989; Capobianco et al., 1990). However, the magnetic dipole transition of F_1 is allowed and is insensitive to the surroundings of the Eu^{3+} ion, so that it is usually utilized as an internal standard. For example, as the ratio of F_2 luminescence intensity to F_1 intensity (RI2) becomes large, the binding site of the Eu^{3+} ion becomes less symmetrical, less polar, and more covalent (Oomen and van Dongen, 1989).

We have applied Eu(III) luminescence spectroscopy to understand the structural adaptation and stability of sC with respect to the binding of each metal cation and the environment of the respective metal cation-binding sites. Eu^{3+} ion is similar to Ca^{2+} ion in size, so that the Ca^{2+} ion can be replaced with Eu^{3+} ion isomorphically. Our results show that two sites are characteristically quite different from each other, although both of them are well defined and very similar to each other compared with the extremely different environment of the free Eu^{3+} ion. Furthermore, the coordination sphere of the strong site of dispersed sC in solution is different from that of crystalline sC.

MATERIALS AND METHODS

$EuCl_3$ and ^2H_2O were purchased from Aldrich Chemical (Milwaukee, WI), and sC, phenylmethyl sulfonylfluoride, and Trizma ($H_2NC(CH_2OH)_3$) were from Sigma Chemical (St. Louis, MO).

Metal cation-removed sC from the strong binding site as well as from the weak site (dSsC) was prepared by deionizing 0.25 mM sC with 10 mM EDTA. Before the deionization process sC was treated in the pH 7.5 aqueous buffer solution of 1 mM phenylmethylsulfonyl fluoride and 10 mM Trizma overnight to inhibit autolysis. The deionized solution was dialyzed several times in the 10 mM Trizma buffer solution and then lyophilized. The resulting powder was stored below 5°C until use. Metal cation-removed sC from the weak binding site (dWsC) was prepared by the same procedures as dSsC, except for the EDTA concentration (1 mM). Eu^{3+}-added dSsC (Eu-dSsC) and Eu^{3+}-added dWsC (Eu-dWsC) were prepared by adding highly concentrated Eu^{3+} aqueous solution to the respective dSsC and dWsC buffer (pH 7.5) solutions of 10 mM Trizma. Deuterated samples were prepared by using ^2HCl and ^2H_2O instead of ^1HCl and ^1H_2O, respectively.

The concentration of sC was determined by measuring absorbance at 280 nm, where the extinction coefficient is $2.5 \times 10^4\ M^{-1}\ cm^{-1}$ (Genov et al., 1995). To make sure that the substitution of Eu^{3+} for Ca^{2+} does not change the structures and functions of sC notably, we have checked several aspects. The autolysis rate of Eu^{3+}-bound sC is as low as that of Ca^{2+}-bound native sC, which is lower than that of deionized sC. Furthermore, the circular dichroism, as well as the absorption and emission spectra, is apparently not affected by Eu^{3+} exchange, although it is affected by Ca^{2+} deionization. All of the samples were in the pH 7.5 aqueous buffer solution of 10 mM Trizma at room temperature throughout the luminescence measurements.

Static luminescence spectra were measured with a homemade fluorometer, which consists of a 350-W Xe lamp (LPS255HR; Schoffel), 0.25-m excitation (GM252; Kratos) and 0.275-m emission (Spectrapro275; Acton Research) monochromators, and a photomultiplier tube (R926; Hamamatsu). All of the static and time-resolved luminescence spectra reported here were measured from front surface excitation at 393 nm and were not corrected for the wavelength-dependent variation of detector sensitivity. Samples were excited with 0.5-ns pulses from a dye laser (LN102; Laser Photonics) pumped by a nitrogen laser (LN1000; Laser Photonics) for time-resolved spectra and decay kinetic profiles. For time-resolved spectra, luminescence was focused into a 0.5-m spectrometer (Spectrapro500; Acton Research) coupled with an intensified CCD (ICCD-576-G; Princeton Instruments). For kinetic profiles, emission was collected into a 0.25-m monochromator (33-86-79; Bausch and Lomb) and detected with a photomultiplier tube (R928; Hamamatsu) connected to a digital oscilloscope (TDS350; Tektronix). The relative trigger times between the laser and the detector were adjusted with a delay/pulse generator (DG535; Stanford Research Systems).

RESULTS AND DISCUSSION

The feature of Eu^{3+} luminescence spectrum changes very significantly as the binding environment changes from sC-free buffer solution to sC-containing solution (Fig. 2). The intensity of F_2 luminescence relative to F_1 luminescence increases dramatically with binding to the enzyme (Table 1). This indicates that both binding sites of sC are much less symmetrical than the binding environment of Eu^{3+} in sC-free solution (Oomen and van Dongen, 1989). The F_2 spectral bandwidths of Eu-dWsC and Eu-dSsC are much narrower than that of Eu^{3+} in sC-free solution, indicating that Eu^{3+} ions with the enzyme are located in well-defined sites. Although the spectra i and ii are similar in the values of RI2 and the F_2 bandwidth, they are significantly different in the wavelength of the F_2 intensity maximum. The relatively blue shift of i by 1.5 nm suggests that the binding environment of Eu^{3+} ion at the weak binding site (Eu(W)) is significantly less polar than that of Eu^{3+} ion at the strong binding site (Eu(S)) (El'yashevich, 1953). However, the F_2 spectrum shows that the environment of Eu(S) is as polar as that of Eu^{3+} in sC-free solution. The polar environment of Eu(S) is supported by the x-ray structure, in which the coordination sphere of the strong site includes a carboxylate group (Bode et al., 1987; McPhalen and James, 1988).

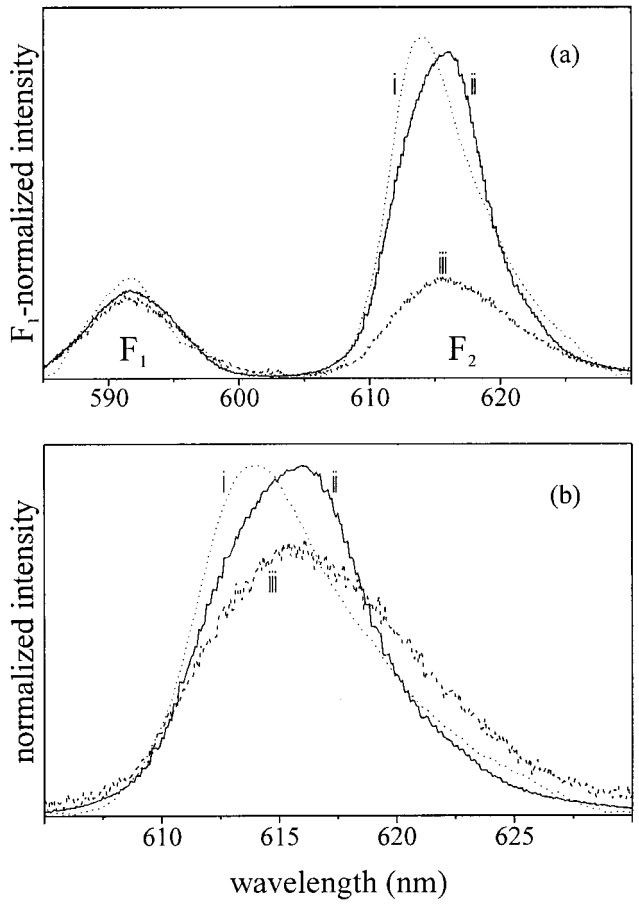

FIGURE 2 F_1-normalized (*a*) and F_2-normalized (*b*) luminescence spectra of 0.25 mM Eu^{3+} in the aqueous buffer (pH 7.5) solutions of 10 mM Trizma. The spectra i and ii were measured with 0.25 mM dWsC and 0.25 mM dSsC, respectively, and iii was measured without sC.

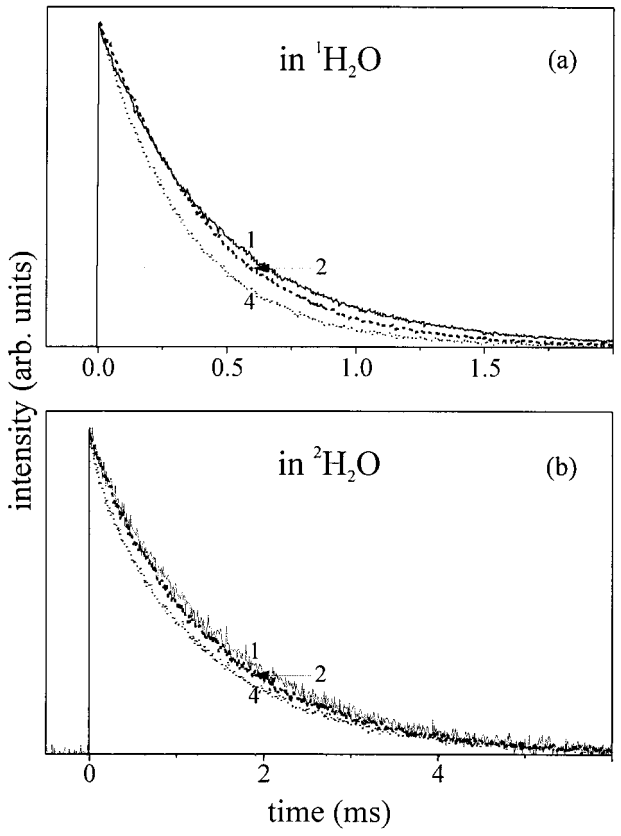

FIGURE 3 Luminescence decay profiles at 617 nm of Eu^{3+} in the ^1H_2O (*a*) and ^2H_2O (*b*) buffer solutions of 0.4 mM dSsC and 10 mM Trizma. The molar concentration ratios of Eu^{3+} to dSsC are indicated by the numbers 1, 2, and 4.

The Eu(III) luminescence decay kinetic profile of Eu-dSsC becomes faster and fits into a more multiple exponential decay as the molar concentration ratio of Eu^{3+} to sC increases (Fig. 3 *a* and Table 2). As the molar ratio of Eu^{3+} to dSsC increases, luminescence from Eu^{3+} bound at the weak binding site as well as that from free Eu^{3+} in the buffer solution admixes with luminescence from Eu^{3+} bound at the strong binding site. This makes the decay profile more complex. The profile fits well into a single exponential decay with a decay time of 480 μs when the molar ratio of Eu^{3+} to sC is 1. However, it fits into a double-exponential decay with decay times of 480 and 350 μs at a molar ratio of 2 and into a triple-exponential decay with decay times of 480, 350, and 160 μs at a molar ratio of 4. The times of 480 and 350 μs are ascribed to the lumi-

TABLE 1 Eu(III) luminescence spectral values of Fig. 2

					F_2 spectrum (nm)	
Spectrum	Sample	[sC]/[Eu]	[sC]/[M]*	RI2	Maximum	FWHM
i	Eu-dWsC	1	0.5	4.1	614.2	7.7
ii	Eu-dSsC	1	1	3.8	615.7	7.7
iii	sC-free	0	0	1.6	615.7	10.8

*Total molar concentration of Ca^{2+} and Eu^{3+}.

TABLE 2 Eu(III) luminescence decay kinetic constants* of Eu-dSsC

		Decay time (μs)		
$[Eu^{3+}]/[sC]$	Solvent	Slow	Medium	Fast
1		480		
2	^1H_2O	480 (51%)†	350	
4		480 (40%)	350 (25%)	160
1		1500		
2	^2H_2O	1500 (51%)	1200	
4		1500 (40%)	1200 (25%)	740
Water coordination number‡		1.5	2.1	5.1

*Extracted from the decay profiles of Fig. 3.
†The relative percent amplitude of each decay component.
‡The number of water molecules coordinated to the Eu^{3+} ion responsible for each decay component was calculated following the method of Horrocks et al. (1981).

nescence decays of Eu(S) and Eu(W), respectively, and the time of 160 μs is ascribed to the luminescence decay of free Eu^{3+} ion surrounded by Trizma and water molecules. A faster decay time implies that there exists a faster vibrational deexcitation pathway; in other words, Eu^{3+} ion is coordinated to more water molecules or amine groups. OH and NH oscillators are known to be the most effective quenchers of Eu(III) luminescence because of their high vibrational frequencies (Beeby et al., 1999). The relative amplitude of the 480-μs component is 40% at a molar ratio of 4, and this is significantly higher than the possible relative presence of 25% for Eu(S). The relative amplitude depends not only on a relative concentration but also on a relative oscillator strength. High relative emission amplitudes for Eu^{3+} bound in the enzyme suggest that the binding sites are less symmetrical than the binding environment of free Eu^{3+} ion outside the enzyme, as shown already with Fig. 1. In particular, Ca^{2+} ion in the strong binding site is reported by x-ray crystallographic studies (Bode et al., 1987; McPhalen and James, 1988) to exist in the center of an almost regular octahedron formed by oxygen ligands. However, the large F_2 oscillator strength and the large RI2 value dictate that the symmetry of the strong binding site is significantly lower than that of an octahedral group.

Replacement of O^1H oscillators in the first coordination sphere by O^2H oscillators causes the vibronic deexcitation pathway to become exceedingly inefficient (Fig. 3 *b*). This fact has enabled us to determine the number of water molecules coordinated to a Eu^{3+} ion, following Horrocks et al. (1981), as

water coordination number

$$= 1.05 \text{ ms}[1/\tau(^1H_2O) - 1/\tau(^2H_2O)] \quad (1)$$

where τ is the decay time of each component. We have fitted the decay kinetic profiles with the assumption that the relative amplitude of each component does not change with the isotope exchange of hydrogen atom. Based on luminescence quenching dynamics, the Eu^{3+} ions at the strong and weak binding sites are found to be coordinated with 1.5 and 2.1 water molecules, respectively, whereas free Eu^{3+} ion is coordinated to 5.1 water molecules.

Because the binding constant of the strong site is much larger than that of the weak site, we have replaced only the Ca^{2+} ion in the weak binding site with a Eu^{3+} ion to check the results from Fig. 3. The medium and fast decay times as well as the resulting water coordination numbers should be reasonably reproducible. Furthermore, we can monitor the luminescence from the weak site without interference from the luminescence from the strong site, so that we can understand the characteristics of the weak site better. The luminescence lifetime and water coordination number of Eu(W), obtained with Fig. 4 and shown in Table 3, are, respectively, the same within experimental error as those in Table 2. The values of free Eu^{3+} in the two tables are also

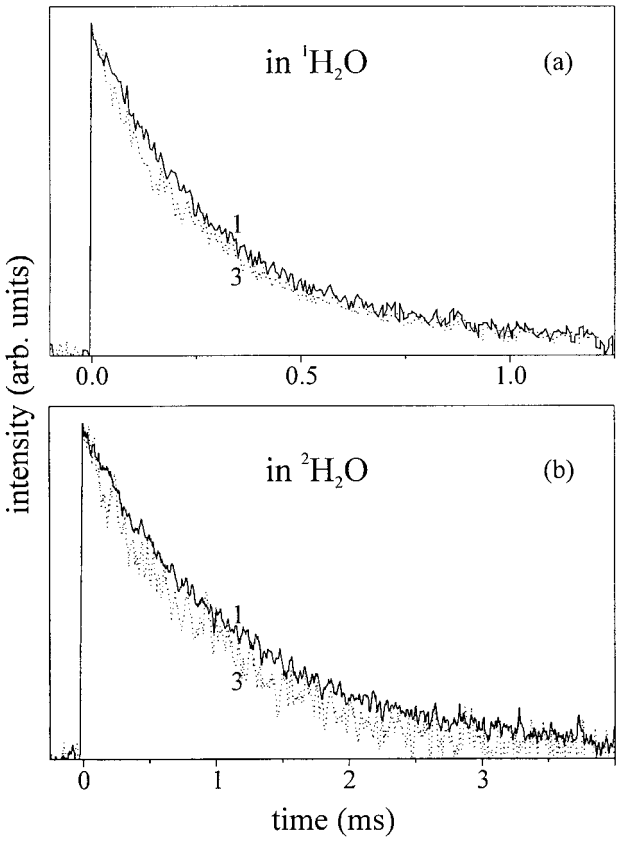

FIGURE 4 Luminescence decay profiles at 617 nm of Eu^{3+} in the ^1H_2O (*a*) and ^2H_2O (*b*) buffer solutions of 0.4 mM dSsC and 10 mM Trizma. The molar concentration ratios of Eu^{3+} to dWsC are indicated by the numbers 1 and 3.

respectively the same. These facts indicate that our data are reasonably good.

Aqueous Eu^{3+} ion is reported to have a water coordination number of ~8–9 and a luminescence decay time of 110 μs (Horrocks and Sudnick, 1981). Then free Eu^{3+} responsible for the fast component has a substantially longer luminescence decay time and a smaller water coordination number than aqueous Eu^{3+}. This is due to the coordination

TABLE 3 Eu(III) luminescence decay kinetic constants* of Eu-dWsC

			Decay time (μs)		
$[Eu^{3+}]/[sC]$	[M]/[sC]	Solvent	Slow	Medium	Fast
1	2	^1H_2O		350	
3	4			350 (60%)	160
1	2	^1H_2O		1200	
3	4			1200 (60%)	740
Water coordination number†				2.1	5.1

*Extracted from the decay profiles of Fig. 4.
†Calculated following the method of Horrocks et al. (1981).

of free Eu^{3+} ion to Trizma molecules as well as to water molecules. The water coordination number of 2.1 for Eu(W) approximately matches that of the two coordinated water molecules found in the x-ray structure (Bode et al., 1987). However, the result that the water coordination number of Eu(S) is 1.5 hardly corresponds with the x-ray report that the first coordination sphere of the strong binding site does not include water molecules at all. It is noteworthy that the water coordination number observed with Eu(III) luminescence quenching dynamics is the upper limit of the actual number because luminescence quenching by any oscillators involving protic hydrogen atoms slows down with deuterium exchange as well. Thus we should correct the contribution of NH oscillators in the number of water coordination. It is more recently reported by Beeby et al. (1999) that an amide NH oscillator bound to a coordinated carbonyl carbon contributes to the hydrogen isotope exchange effect on Eu(III) luminescence quenching as much as 0.079 water molecule does. On the other hand, a coordinated NH oscillator contributes at least as much as half of a water molecule does, that is, one OH oscillator, although the actual extent depends on the situation.

Then the coordination of free Eu^{3+} is the total coordination number of water and Trizma molecules, as the coordination of a Trizma molecule would have about the same effect as the coordination of one water molecule. Considering the coordination number of 5 and the bulky structure of the Trizma molecule, we suggest a triangular bipyramidal structure with a Trizma molecule at the apex of each pyramid as the coordination structure of free Eu^{3+}. Considering the additional effect of three carbonyl-bound amide NH oscillators and the reduced effect of the hydrogen bonding of coordinated waters to carboxylate groups (Bode et al., 1987; McPhalen and James, 1988), the water coordination number in the weak site is 2, as found from the x-ray studies. However, the correction of the contribution of seven carbonyl-bound amide NH oscillators (Beeby et al., 1999) leaves one water molecule as the ligand for the strong site, whereas no coordinated water is found in the x-ray structure. Considering this discrepancy, we suggest that a metal cation at the strong site is coordinately bound to a water molecule in the aqueous solution, whereas it is not in the crystalline structure. However, it could be possible that a disordered water molecule is present near the strong site in the crystalline structure as well, because it is generally difficult to detect water molecules in x-ray studies. One may also point out that the water coordination of Eu(S) is due to the larger coordination number of a Eu^{3+} ion than of a Ca^{2+} ion in general. This is not considered seriously, as Eu(W) does not have any additionally coordinated water molecules.

Fig. 5 illustrates that two sites are characteristically significantly different from each other. The RI2 value increases monotonically with time in Fig. 5, *a* and *c*. In Fig. 5 *b*, however, it increases at 300 μs but then decreases at 800 μs. The emission of free Eu^{3+} with the shortest lifetime contributes significantly to make the RI2 value smaller early. RI2 increases monotonically with time in Fig. 5, *a* and *c*, because both Eu(S) and Eu(W) have significantly longer emission lifetimes with much larger RI2 values than free Eu^{3+}; besides free Eu^{3+} ions floating in the solution, basically Eu^{3+} ions are bound to only the strong site in Fig. 5 *a* and to only the weak site in Fig. 5 *c*. RI2 value, however, increases and then decreases with time in Fig. 5 *b*, where both the strong and weak sites are occupied by Eu^{3+} ions. This is because Eu(S) has a longer lifetime but a smaller RI2 value than Eu(W). The spectral width of the F_2 band becomes narrower early, as luminescence from Eu^{3+} bound in the well-defined sites of the enzyme has narrower widths

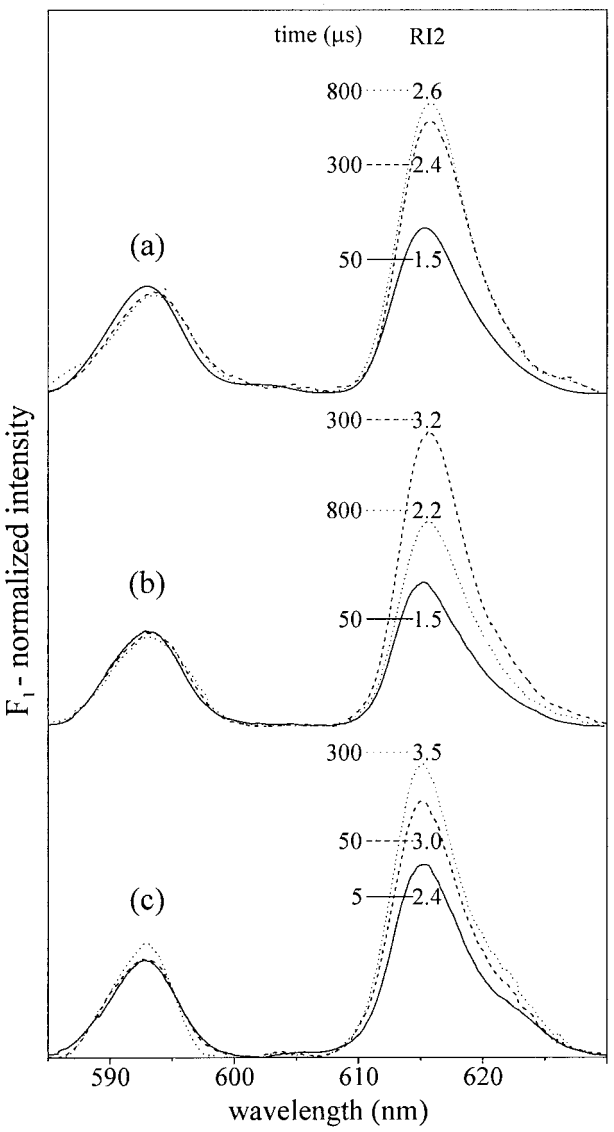

FIGURE 5 F_1-normalized time-resolved luminescence spectra of the 10 mM Trizma buffer solutions of 0.25 mM Eu^{3+} and 0.25 mM dSsC (*a*), 0.50 mM Eu^{3+} and 0.25 mM dSsC (*b*), and 0.25 mM Eu^{3+} and 0.25 mM dWsC (*c*). The delay times and RI2 values of the respective spectra are indicated.

TABLE 4 Characteristic comparison of Eu(S), Eu(W), and free Eu^{3+} in 10 mM Trizma aqueous buffer (pH 7.5) solution

	Eu(S)	Eu(W)	Free Eu^{3+}
Peak wavelength of F_2 (nm)	615.7	614.2	615.7
FWHM of F_2 (nm)	6.5	6.5	10.8
RI2	3.8	4.1	1.6
Emission lifetime in ^1H_2O (μs)	480	350	160
Emission lifetime in ^2H_2O (μs)	1500	1200	740
Water coordination number*	1	2	5†
Binding site symmetry	Less symmetrical	Least symmetrical	Symmetrical
Binding site polarity	Polar	Less polar	Polar

*Calculated with the correction of carbonyl-bound amide NH oscillator effect, following the method of Beeby et al. (1999).
†The total coordination number of water and Trizma molecules.

with longer lifetimes than luminescence from free Eu^{3+} in the solution. However, the widths in Fig. 5 become similar to each other in the long delay time domain after excitation, as Eu(S) and Eu(W) are found to have about the same widths. The full width at half-maximum F_2 bandwidths of Eu(S) and Eu(W) are 6.5 nm, which is much smaller than the width (10.8 nm) of free Eu^{3+} given in Table 1. This fact again shows that Eu(W) as well as Eu(S) is located in a well-defined position. The F_2 bandwidths of the static spectra i and ii in Fig. 2 are significantly broader than those from the time-resolved spectra of Fig. 5. This is due to the luminescence interference from free Eu^{3+} in the static spectra of Fig. 2. Fig. 5 also shows that the spectrum at 300 μs of Fig. 5 *c* is shifted to the blue compared with the spectrum at 300 μs of Fig. 5 *a*. This indicates that Eu(S) is located in a relatively more polar environment than Eu(W), as suggested by Fig. 2.

Table 4 compares the experimentally observed characteristics of Eu(S), Eu(W), and free Eu^{3+}. The peak wavelengths of F_2 are from Table 1, because a static measurement is technically more accurate in wavelength than is a time-resolved method, and a slight spectral contamination effect by luminescence from free Eu^{3+} would be negligible for the determination of the peak wavelength. The bandwidths of F_2 are from Fig. 5, as luminescence from free Eu^{3+} would contribute negligibly to emission intensity at long delay times. RI2 values are from Table 1, for the numbers in Table 1 are still the low limits of actual RI2 values and they are higher than any values of Fig. 5. The other values in Table 4 are unambiguously extracted from the respective results already presented.

The F_2 band of Eu(S) is significantly redder than that of Eu(W) and about the same as that of free Eu^{3+}. This suggests that the environment of Eu(S) is much polar than that of Eu(W) and even as polar as that of free Eu^{3+} (El'yashevich, 1953). This agrees with the fact that only Eu(S) has a charged coordination group (Bode et al., 1987). The narrow F_2 bandwidths of Eu(S) and Eu(W), compared with the width of free Eu^{3+}, are attributable to the well-defined binding structures of both sites. High RI2 values are due to the significantly lower symmetry of the two sites compared with the coordination environment of free Eu^{3+}. Considering the high RI2 values together with the high relative oscillator strengths of Table 2, the F_2 transition of Eu^{3+} at both binding sites is first-order allowed. This implies that the coordination symmetry groups of both sites have neither an inversion center nor a horizontal mirror plane (Parsapour et al., 1998). The higher RI2 value suggests that Eu(W) has an even less symmetrical binding environment than Eu(S). The luminescence lifetime and its variation with hydrogen isotope exchange are determined by the water coordination number as well as by the carbonyl-bound amide NH oscillators, as already described. While the water coordination number 2 of the weak site matches the number found in the x-ray crystalline structure, that of the strong site is 1, despite the zero value in the crystalline structure. This indicates that the weak site is not easily accessible to solvent or substrate once it is bound to a metal cation. On the other hand, the strong site is accessible to a solvent or substrate molecule. Our results cannot tell directly whether a water molecule binds to the metal cation at the strong site instead of a coordinated group or in addition to the ligands present in the crystalline structure. Considering the binding constant, which is larger by a factor of 10^6 than that of the weak site (Pantoliano et al., 1989), we infer that a water molecule binds additionally in aqueous solution to a metal cation at the strong site. The additional coordination of Ca^{2+} at the strong site with a solvent molecule or a substrate molecule could indicate that the binding of a metal cation to the strong site plays an important functional role during the catalytic reaction of the enzyme. This is in addition to the known structural role of Ca^{2+} binding, in which it enhances the thermal and chemical stability of the enzyme (Genov et al., 1995; Kidd et al., 1996; Pantoliano et al., 1988; Strausberg et al., 1995; Voordouw et al., 1976). The coordination of Ca^{2+} at the strong site with a substrate molecule, if it occurs, would enhance the conformational stability of the enzyme-substrate complex intermediate necessary for the catalytic function.

CONCLUSION

Eu^{3+} has been isomorphically and selectively substituted for Ca^{2+} in the two cation-binding sites of serine endopep-

tidase sC, and its time-resolved and static luminescence has been probed to characterize the surroundings of Eu^{3+} bound in the respective sites. Although two binding sites are characteristically quite different from each other, they are very similar to each other compared with the coordination sphere of free Eu^{3+} ion. Thus both sites have a well-defined binding structure with low coordination symmetry, although the strong site is more polar, more symmetrical, and more approachable than the weak site. Furthermore, despite the fact that no water is found in the x-ray crystal structure (Bode et al., 1987), one water molecule is found to exist in the first coordination sphere of the strong site in our experiment. Thus we suggest that the Ca^{2+} ion bound in the strong site binds to a solvent or substrate molecule by forming an additional coordination bond in solution. It is further inferred that the binding of Ca^{2+} ion to the strong site plays an important role in the catalytic function of the enzyme as well as in the thermal and chemical stability of the protein structure.

We thank the Center for Molecular Catalysis and the Basic Science Research Institute Program for financial support. SL acknowledges the fellowship from the Brain Korea 21 Program.

REFERENCES

Beeby, A., I. M. Clarkson, R. S. Dickins, S. Faulkner, D. Parker, L. Royle, A. S. de Sousa, J. A. G. Williams, and M. Woods. 1999. Non-radiative deactivation of the excited states of europium, terbium and ytterbium complexes by proximate energy-matched OH, NH and CH oscillators: an improved luminescence method for establishing solution hydration states. *J. Chem. Soc. Perkin Trans.* 2:493–503.

Bode, W., E. Papamokos, and D. Musil. 1987. The high-resolution x-ray crystal structure of the complex formed between subtilisin Carlsberg and eglin c, an elastase inhibitor from the leech *Hirudo medicinalis*. *Eur. J. Biochem.* 166:673–692.

Broos, J., A. J. W. G. Visser, J. F. J. Engbersen, W. Verboom, A. van Hoek, and D. N. Reinhoudt. 1995. Flexibility of enzymes suspended in organic solvents probed by time-resolved fluorescence anisotropy. Evidence that enzyme activity and enantioselectivity are directly related to enzyme flexibility. *J. Am. Chem. Soc.* 117:12657–12663.

Bunzli, J.-C. G., and G. R. Choppin. 1989. Lanthanide Probes in Life, Chemical and Earth Sciences. Elsevier Science, Amsterdam.

Capobianco, J. A., P. P. Proulx, M. Bettinelli, and F. Negrisolo. 1990. Absorption and emission spectroscopy of Eu^{3+} in metaphosphate glasses. *Phys. Rev. B.* 42:5936–5944.

Carter, P., and J. A. Wells. 1988. Dissecting the catalytic triad of a serine protease. *Nature.* 332:564–568.

Chatterjee, S., and A. J. Russell. 1993. Kinetic analysis of the mechanism for subtilisin in essentially anhydrous organic solvents. *Enzyme Microb. Technol.* 15:1022–1029.

Chaudhary, A. K., S. V. Kamat, E. J. Beckman, D. Nurok, R. M. Kleyle, P. Hajdu, and A. J. Russell. 1996. Control of subtilisin substrate specificity by solvent engineering in organic solvents and supercritical fluoroform. *J. Am. Chem. Soc.* 118:12891–12901.

Choppin, G. R., and D. R. Peterman. 1998. Applications of lanthanide luminescence spectroscopy to solution studies of coordination chemistry. *Coord. Chem. Rev.* 174:283–299.

El'yashevich, M. A. 1953. Spectra of the Rare Earths. State Publishing House of Technical-Theoretical Literature, Moscow. 497–512.

Fitzpatrick, P. A., D. Ringe, and A. M. Klibanov. 1994. X-ray crystal structure of cross-linked subtilisin Carlsberg in water vs. acetonitrile. *Biochem. Biophys. Res. Commun.* 198:675–681.

Genov, N., B. Filippi, P. Dolashka, K. S. Wilson, and C. Betzel. 1995. Stability of subtilisin and related proteinases (subtilases). *Int. J. Pept. Protein Res.* 45:391–400.

Horrocks, W. D., Jr., and D. R. Sudnick. 1981. Lanthanide ion luminescence probes of the structure of biological macromolecules. *Acc. Chem. Res.* 14:384–392.

Kidd, R. D., H. P. Yennawar, P. Sears, C.-H. Wong, and G. K. Farber. 1996. A weak calcium binding site in subtilisin BPN′ has a dramatic effect on protein stability. *J. Am. Chem. Soc.* 118:1645–1650.

Kijima, T., S. Yamamoto, and H. Kise. 1994. Fluorescence spectroscopic study of subtilisins as relevant to their catalytic activity in aqueous-organic media. *Bull. Chem. Soc. Jpn.* 67:2819–2824.

Lee, S., H. Hwang, P. Kim, and D.-J. Jang. 1999. Time-resolved Eu luminescence spectra and kinetics at various Y zeolitic environments. *Catal. Lett.* 57:221–226.

McPhalen, C. A., and M. N. G. James. 1988. Structural comparison of two serine proteinase-protein inhibitor complexes: eglin-c-subtilisin Carlsberg and CI-2-subtilisin Novo. *Biochemistry.* 27:6582–6598.

Neidhart, D. J., and G. A. Petsko. 1988. The refined crystal structure of subtilisin Carlsberg at 2.5 Å resolution. *Protein Eng.* 2:271–276.

Oomen, E. W. J. L., and A. M. A. van Dongen. 1989. Europium (III) in oxide glasses: dependence of the emission spectrum upon glass composition. *J. Non-Cryst. Sol.* 111:205–213.

Pantoliano, M. W., M. Whitlow, J. F. Wood, S. W. Dodd, K. D. Hardman, M. L. Rollence, and P. N. Bryan. 1989. Large increases in general stability for subtilisin BPN′ through incremental changes in the free energy of unfolding. *Biochemistry.* 28:7205–7213.

Pantoliano, M. W., M. Whitlow, J. F. Wood, M. L. Rollence, B. C. Finzel, G. L. Gilliland, T. L. Poulos, and P. N. Bryan. 1988. The engineering of binding affinity at metal ion binding sites for the stabilization of proteins: subtilisin as a test case. *Biochemistry.* 27:8311–8317.

Parsapour, F., D. F. Kelley, and R. S. Williams. 1998. Spectroscopy of Eu^{3+}-doped PtS_2 nanoclusters. *J. Phys. Chem. B.* 102:7971–7977.

Pucker, G., K. Gatterer, H. P. Fritzer, M. Bettinelli, and M. Ferrari. 1996. Optical investigation of Eu^{3+} in a sodium borosilicate glass: evidence for two different site distributions. *Phys. Rev. B.* 53:6225–6234.

Siezen, R. J., W. M. de Vos, J. A. M. Leunissen, and B. W. Dijkstra. 1991. Homology modelling and protein engineering strategy of subtilases, the family of subtilisin-like serine proteinases. *Protein Eng.* 4:719–737.

Smith, E. L., R. J. Delange, W. H. Evans, M. Landon, and F. S. Markland. 1968. Subtilisin Carlsberg. V. The complete sequence; comparison with subtilisin BPN′; evolutionary relationships. *J. Biol. Chem.* 243: 2184–2191.

Strausberg, S., P. A. Alexander, D. T. Gallagher, G. L. Gilliland, B. L. Barnett, and P. N. Bryan. 1995. Directed evolution of a subtilisin with calcium-independent stability. *Biotechnology (NY).* 13:669–673.

Strausberg, S., P. Alexander, L. Wang, T. Gallagher, G. Gilliland, and P. Bryan. 1993. An engineered disulfide cross-link accelerates the refolding rate of calcium-free subtilisin by 850-fold. *Biochemistry.* 32: 10371–10377.

Voordouw, G., C. Milo, and R. S. Roche. 1976. Role of bound calcium ions in thermostable, proteolytic enzymes. Separation of intrinsic and calcium ion contributions to the kinetic thermal stability. *Biochemistry.* 15:3716–3724.